2010 IEEE International Conference on Robotics and Automation
Anchorage Convention District
May 3-8, 2010, Anchorage, Alaska, USA

Improving Stability and Performance of Digitally Controlled Systems: the Concept of Modified Holds

Kamran Ghaffari Toiserkan and József Kövecses

Abstract—**Digitally controlled systems are getting more and more popular mainly because of their flexibility and convenience but their stability is strongly affected by the time delay introduced by different factors. For common PID type digital controllers, zero-order holds (ZOHs) are commonly employed and the stability characteristics are investigated based on that concept. Mathematical investigations show that higher-order holds may improve the stability and performance of the system and can reduce the steady state errors significantly. This is because the controller tries to learn from the history of the behavior of the system and then predict the behavior for the time period between sampling instances and generate the best possible control force. Furthermore, a new concept of Modified Holds is introduced, which clearly improves the performance of a digital controller. For most control algorithms this does not prolong the processing time significantly (e.g. less than 1%) which can be neglected in the calculations. The varying control force would need an analogue circuitry to follow the proper curve, which might make the controller's electronic circuits more complex. This can be avoided considering that in almost all digital controllers the main core operates at several orders of magnitude higher frequency than that of the control loop itself. Hence, the control force can also be generated digitally at much higher frequencies. In this paper, after investigating the stability of a 1-DoF system equipped with discrete-time PD controller with first and second order holds, the concept of modified holds is introduced and then the results are validated by simulations. Furthermore, the concept is practically implemented on a self-balancing motor bike robot and the experimental results further support the claims of the paper.**

I. Introduction

Stability is one of the most important aspects of a controlled system. Digitally controlled systems are increasingly used, but their stability is strongly affected by the time delay mainly introduced by data processing. In discrete-time controllers the time delay dictates limits for the value of proportional gain as apposed to continuous time controllers, where, ideally, the only limit for the proportional gain is the power capability of the actuators [1]-[3]. This in turn affects the performance of the system. Common PID-type digital controllers employ zero-order holds (ZOHs). In these systems, a proper control force is calculated for each time step t_j , and its value is kept constant until the next sampling time t_{j+1}. Higher order holds consider a longer history of the system outputs to generate a time varying control force during each sampling period. This is done by predicting the future behavior based on the previous rate of change of the system outputs. Fig. 1, illustrates how the control force is generated by using the slope of the line connecting the two previous states in a first-order-hold (FOH). Consequently, a second-order-hold (SOH) generates a nonlinear force profile using the curvature and the slope obtained from the three previous states of the system. There have been several different approaches to improve the stability and performance of digital controllers e.g. [9]-[12]. In this paper, we investigate how higher-order holds affect the stability of digitally controlled systems, and if any modification can be applied to this concept to improve the stability and performance. This concept can be used to improve the control of various types of systems (e.g. position/force controlled) especially if the system does not suffer from large random disturbances. The mathematical approach in this paper is introduced based on using a 1-DoF position controlled system, but it can be easily expanded to multi degree of freedom force feedback devices as well.

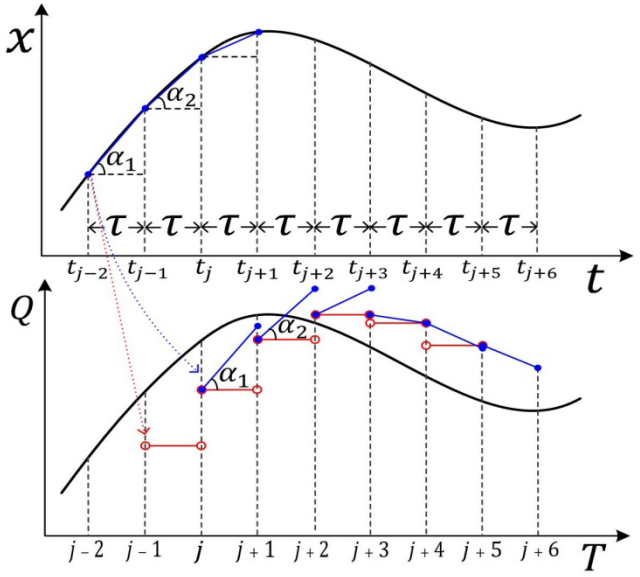

Fig. 1. FOH uses the slope of the line connecting the previous two steps of state variables as a reference to generate a proper force during the next sampling time τ (blue lines). In case of a ZOH the control force is kept constant proportionally with the last measured state (red lines).

II. Stability Analysis using FOH

Position controlled robots have a broad range of applications. There have been a lot of efforts to increase the stability, precision and robustness of these systems, which would require high performance processors and more advanced sensors and electronic circuits.

Both authors are with the Department of Mechanical Engineering and Centre for Intelligent Machines, McGill University, Montreal, Quebec, Canada, (e-mails: kamran@cim.mcgill.ca and jozsef.kovecses@mcgill.ca)

Let us consider a 1-DoF system (Fig. 2), and we would like to control its position to move it from point A to point B in the presence of Coulomb friction. A common solution would be to use PD controller strategy to generate a proper force to simulate a virtual spring/damper setup connected to the system in study. This system can be modeled as it is shown in Fig. 2. The equation of motion of the system is derived as:

$$m\ddot{q}(t) = Q(t) - Csgn\left(\dot{q}(t)\right) \tag{1}$$

where $Q(t)$ represents the control force and $Csgn(\dot{q}(t))$ is the Coulomb friction force. Let us define a second coordinate x associated with the position error originated at point B. As q and x coordinates are aligned it's clear that:

$$\ddot{q}(t) = \ddot{x}(t)\,,\ \dot{q}(t) = \dot{x}(t) \tag{2}$$

For PD controllers $Q(t)$ is calculated based on the linear combination of the error and its derivative for each DoF. In discrete time controllers, we are dealing with time delays arose from measuring the states of the system, computational processing and some other factors. The effect of such time delays in the behavior of the system has been investigated in the recent literature [1],[2],[8]. In these controllers, until a new control force profile is defined and is ready to be applied to the system, at least one sampling period is elapsed. In other words, at every sampling instance a new control force function is defined based on the data acquired in the past and will be kept valid until the next sampling period, as there is no real-time information from the output of the system during a sampling interval. In case of a ZOH, the value of $Q(t)$ is kept constant for the entire sampling period (see Fig. 1). Therefore, the effective $Q(t)$ at any time $t \in [t_j, t_{j+1})$ can be considered as:

$$Q(t) = -Px\left(t_{j-1}\right) - D\dot{x}(t_{j-1}) \tag{3}$$

where P and D are proportional and differential gains, respectively. A FOH can interpret a linearly varying force profile in each sampling period, where the slope is obtained from the slope of the error line in the last two steps using Euler's backward method (i.e. $[x\,(t_{j-1}) - x(t_{j-2})]/\tau$). This results in a control force

$$\begin{aligned} Q(t) = &-P\left[x(t_{j-1}) + \left(\frac{x(t_{j-1})-x(t_{j-2})}{\tau}\right)(t-t_j)\right] \\ &-D\left[\dot{x}(t_{j-1}) + \left(\frac{\dot{x}(t_{j-1})-\dot{x}(t_{j-2})}{\tau}\right)(t-t_j)\right] \end{aligned} \tag{4}$$

Now combining (1), (2) and (4) we get the equation of motion of the controlled system in the time domain.

$$\begin{aligned} m\ddot{x}(t) = &-P\left[x(t_{j-1}) + \left(\frac{x(t_{j-1})-x(t_{j-2})}{\tau}\right)(t-t_j)\right] \\ &-D\left[\dot{x}(t_{j-1}) + \left(\frac{\dot{x}(t_{j-1})-\dot{x}(t_{j-2})}{\tau}\right)(t-t_j)\right] - Csgn(\dot{x}(t)) \end{aligned} \tag{5}$$

The steady state error is a result of Coulomb friction where $|\Delta x_{\min}| = \frac{C}{P}$ which clearly shows that larger proportional gains in the stability domain reduce the steady state error. On the other hand, friction dissipates energy which has a stabilizing effect on the system. Hence, for the stability analysis, we consider the conservative case of a frictionless system.

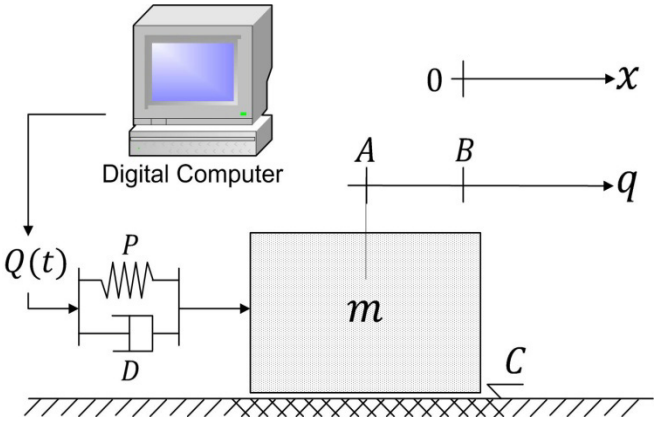

Fig. 2. Model of a computer controlled 1-DoF system in presence of Coulomb friction. PD controller can be modeled as a virtual spring/dashpot.

Let us now introduce the dimensionless time: $T = t/\tau$. Thus, at time $t = t_j$ we have $T = \frac{j\tau}{\tau} = j$. Also, upon the chain rule we have $\frac{1}{\tau}\frac{d}{dT} = \frac{d}{dt} \rightarrow \frac{1}{\tau}\square' = \dot{\square}$. Therefore, (5) can be mapped into the dimensionless time domain as:

$$\begin{aligned} x''(T) = &-\frac{P\tau^2}{m}\left[x_{j-1} + (x_{j-1} - x_{j-2})(T-j)\right] \\ &-\frac{D\tau}{m}\left[x'_{j-1} + (x'_{j-1} - x'_{j-2})(T-j)\right] \end{aligned} \tag{6}$$

For the sake of simplicity let's define new dimensionless gains: $p = P\tau^2/m$, $d = D\tau/m$ and substitute them into (6). The first differentiation of (6) gives us the slope of the control force which is the rate of change of the acceleration of the system and is constant during each sampling period. For time period $t \in [t_j, t_{j+1})$ we can write:

$$x'''(T) = x'''(j) = -p(x_{j-1} - x_{j-2}) - d(x'_{j-1} - x'_{j-2}) \tag{7}$$

The solution of (6) can be obtained by integration as:

$$\begin{aligned} x'(T) = &-p\left[\left((1-j)x_{j-1} + jx_{j-2}\right)T + \frac{1}{2}\left(x_{j-1} - x_{j-2}\right)T^2\right] \\ &-d\left[\left((1-j)x'_{j-1} + jx'_{j-2}\right)T + \frac{1}{2}\left(x'_{j-1} - x'_{j-2}\right)T^2\right] + C_1 \end{aligned} \tag{8}$$

$$\begin{aligned} x(T) = &-p\left[\frac{1}{2}\left((1-j)x_{j-1} + jx_{j-2}\right)T^2 + \frac{1}{6}\left(x_{j-1} - x_{j-2}\right)T^3\right] \\ &-d\left[\frac{1}{2}\left((1-j)x'_{j-1} + jx'_{j-2}\right)T^2 + \frac{1}{6}\left(x'_{j-1} - x'_{j-2}\right)T^3\right] + C_1T + C_2 \end{aligned} \tag{9}$$

where C_1 and C_2 are integration constants, which are determined considering the initial conditions at the beginning of the sampling period $T = j$ and turn (8) and (9) into the following form:

$$\begin{aligned} x'(T) = x'(j) &- p\left[(T-j)x_{j-1} + \frac{1}{2}(x_{j-1} - x_{j-2})(T-j)^2\right] \\ &-d\left[(T-j)x'_{j-1} + \frac{1}{2}(x'_{j-1} - x'_{j-2})(T-j)^2\right] \end{aligned} \tag{10}$$

$$x(T) = (T-j)\dot{x}(j) + x(j) - p\left[\tfrac{1}{2}(T-j)^2 x_{j-1} + \tfrac{1}{6}(x_{j-1} - x_{j-2})(T-j)^3\right] - d\left[\tfrac{1}{2}(T-j)^2 \dot{x}_{j-1} + \tfrac{1}{6}(\dot{x}_{j-1} - \dot{x}_{j-2})(T-j)^3\right] \quad (11)$$

Moving to the next sampling time at $T = j+1$ the new state of the system can be expressed as a linear combination of the j^{th} and $(j-1)^{\text{th}}$ states resulting in the following set of difference equations:

$$\dddot{x}(j+1) = -p(x_j - x_{j-1}) - d(\dot{x}_j - \dot{x}_{j-1}) \quad (12.a)$$

$$\ddot{x}(j+1) = -px_j - d\dot{x}_j \quad (12.b)$$

$$\dot{x}(j+1) = \dot{x}(j) + \ddot{x}(j) + \tfrac{1}{2}\dddot{x}(j) \quad (12.c)$$

$$x(j+1) = x(j) + \dot{x}(j) + \tfrac{1}{2}\ddot{x}(j) + \tfrac{1}{6}\dddot{x}(j) \quad (12.d)$$

which can be expressed in to the state space format, as

$$\begin{bmatrix} x(j) \\ \dot{x}(j) \\ x(j+1) \\ \dot{x}(j+1) \\ \ddot{x}(j+1) \\ \dddot{x}(j+1) \end{bmatrix} = \underbrace{\begin{bmatrix} 0 & 0 & 1 & 0 & 0 & 0 \\ 0 & 0 & 0 & 1 & 0 & 0 \\ 0 & 0 & 1 & 1 & 1/2 & 1/6 \\ 0 & 0 & 0 & 1 & 1 & 1/2 \\ 0 & 0 & -p & -d & 0 & 0 \\ p & d & -p & -d & 0 & 0 \end{bmatrix}}_{\boldsymbol{A}} \begin{bmatrix} x(j-1) \\ \dot{x}(j-1) \\ x(j) \\ \dot{x}(j) \\ \ddot{x}(j) \\ \dddot{x}(j) \end{bmatrix} \quad (13)$$

Equation (13) represents a set of geometric series in terms of state variables. These series will converge if and only if the eigenvalues of the state matrix $\boldsymbol{A}$ lie strictly inside the unit circle centered at the origin in the Z-domain. Fig. 3 illustrates the mapping of the continuous dimensionless time system into the unit circle in the Z-domain. The stability margin can be determined either numerically by measuring the absolute value of the maximum eigenvalue of matrix $\boldsymbol{A}$ for sweeping values of the p and d gains, or by applying the Routh-Hurwitz criterion using bilinear mapping. As there is no analytical solution for the eigenvalues of large matrices the second solution can only be applicable to low order systems. If ZOH is used in our analysis, then the last row of matrix $\boldsymbol{A}$ would turn to zero as $\dddot{x}(T) = 0$ all the time. The stability domains for both the ZOH and the FOH cases are presented in Figs. 4 and 5.

At the first look, one would notice that the maximum allowable p gain is increased when FOH is used which can improve the best achievable accuracy. There are other

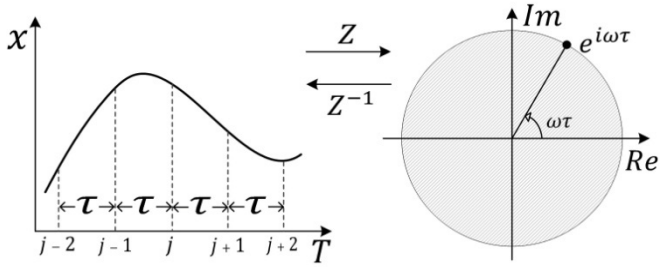

Fig. 3. Mapping between dimensionless time domain and Z-domain via Z and Z^{-1} transformation. ω represents the angular natural frequency of the undamped system.

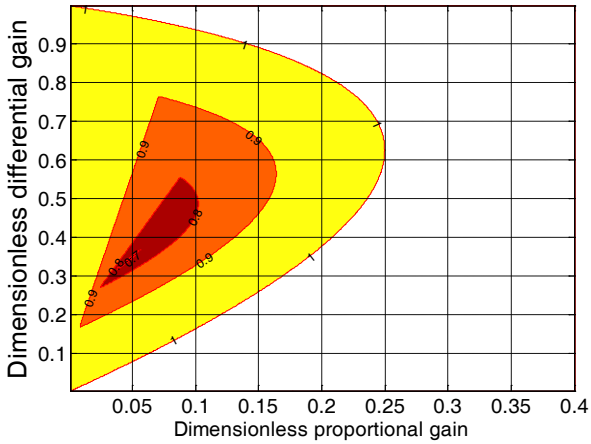

Fig. 4. Stability chart for PD controllers using ZOH. The darker colors represent the more stable zones. The most robust setting is at $p = 0.042$ and $d = 0.32$.

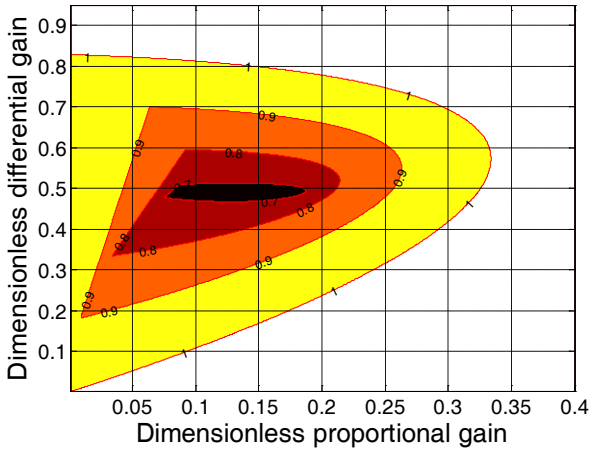

Fig. 5. Stability chart for PD controllers using FOH. The darker colors represent the more stable zones. The most robust setting is at $p = 0.18$ and $d = 0.49$.

interesting areas inside the chart where the least absolute value of the maximum eigenvalue (i.e. spectral radius) of matrix $\boldsymbol{A}$ can be found. This is the zone where we experience the shortest settling time, while the controller is tuned to have the best performance. Interestingly, it can be seen that not only the most robust zone grows in the case of a FOH but also it is shifted to the right, where the p gain is much larger, which results in a smaller steady state error even in the most robust zone (see Fig. 4 and 5). Increasing the maximum allowable p gain could be even more interesting in impedance control applications, where the p gain corresponds to the maximum achievable virtual stiffness. Moreover, improving the performance of the controller increases the transparency between the virtual environment and the haptic device.

III. Stability Analysis using SOH

In case of using a SOH the control force in (1) is represented with a second degree polynomial where the slope and the curvature are determined based on the last three steps. The curvature can be approximated using Euler's backward formula i.e. $[x(t_{j-1}) - 2x(t_{j-2}) + x(t_{j-3})]/\tau^2$

$$Q_{SOH}(t) = -P\left[x(t_{j-1}) + \left(\frac{x(t_{j-1}) - x(t_{j-2})}{\tau}\right)(t - t_j) + \left(\frac{x(t_{j-1}) - 2x(t_{j-2}) + x(t_{j-3})}{\tau^2}\right)(t - t_j)^2\right] - D\left[\dot{x}(t_{j-1}) + \left(\frac{\dot{x}(t_{j-1}) - \dot{x}(t_{j-2})}{\tau}\right)(t - t_j) + \left(\frac{\dot{x}(t_{j-1}) - 2\dot{x}(t_{j-2}) + \dot{x}(t_{j-3})}{\tau^2}\right)(t - t_j)^2\right] \quad (14)$$

Using (14), considering a frictionless system, we can reconstruct (1) in the dimensionless time domain as

$$\ddot{x}(T) = -p\left[x_{j-1} + (x_{j-1} - x_{j-2})(T - j) + (x_{j-1} - 2x_{j-2} + x_{j-3})(T - j)^2\right] - d\left[\dot{x}_{j-1} + (\dot{x}_{j-1} - \dot{x}_{j-2})(T - j) + (\dot{x}_{j-1} - 2\dot{x}_{j-2} + \dot{x}_{j-3})(T - j)^2\right] \quad (15)$$

Following steps similar to the case of a FOH, for the time period $t \in [t_j, t_{j+1})$, results in:

$$\overset{iv}{x}(T) = \overset{iv}{x}(j) = -p\,[2(x_{j-1} - 2x_{j-2} + x_{j-3})] - d[2(\dot{x}_{j-1} - 2\dot{x}_{j-2} + \dot{x}_{j-3})] \quad (16.a)$$

$$\dddot{x}(T) = -p\left[(x_{j-1} - x_{j-2}) + 2(x_{j-1} - 2x_{j-2} + x_{j-3})(T - j)\right] - d\left[(\dot{x}_{j-1} - \dot{x}_{j-2}) + 2(\dot{x}_{j-1} - 2\dot{x}_{j-2} + \dot{x}_{j-3})(T - j)\right] \quad (16.b)$$

$$\dot{x}(T) = \dot{x}(j) - p\left[x_{j-1}(T - j) + \frac{1}{2}(x_{j-1} - x_{j-2})(T - j)^2 + \frac{1}{3}(x_{j-1} - 2x_{j-2} + x_{j-3})(T - j)^3\right] - d\left[\dot{x}_{j-1}(T - j) + \frac{1}{2}(\dot{x}_{j-1} - \dot{x}_{j-2})(T - j)^2 + \frac{1}{3}(\dot{x}_{j-1} - 2\dot{x}_{j-2} + \dot{x}_{j-3})(T - j)^3\right] \quad (16.c)$$

$$x(T) = x(j) + \dot{x}(j)(T - j) - p\left[\frac{1}{2}x_{j-1}(T - j)^2 + \frac{1}{6}(x_{j-1} - x_{j-2})(T - j)^3 + \frac{1}{24}(x_{j-1} - 2x_{j-2} + x_{j-3})(T - j)^4\right] - d\left[\frac{1}{2}\dot{x}_{j-1}(T - j)^2 + \frac{1}{6}(\dot{x}_{j-1} - \dot{x}_{j-2})(T - j)^3 + \frac{1}{24}(\dot{x}_{j-1} - 2\dot{x}_{j-2} + \dot{x}_{j-3})(T - j)^4\right] \quad (16.d)$$

For the next sampling time at $T = j + 1$ the new state of the system can be expressed as the linear combination of the j^{th}, $(j-1)^{\text{th}}$ and $(j-2)^{\text{th}}$ states resulting in the difference equations:

$$\overset{iv}{x}(j+1) = -p[2(x_j - 2x_{j-1} + x_{j-2})] - d[2(\dot{x}_j - 2\dot{x}_{j-1} + \dot{x}_{j-2})] \quad (17.a)$$

$$\dddot{x}(j+1) = -p(x_{j-1} - x_{j-2}) - d(\dot{x}_{j-1} - \dot{x}_{j-2}) \quad (17.b)$$

$$\ddot{x}(j+1) = -px_j - d\dot{x}_j \quad (17.c)$$

$$\dot{x}(j+1) = \dot{x}(j) + \ddot{x}(j) + \frac{1}{2}\dddot{x}(j) + \frac{1}{6}\overset{iv}{x}(j) \quad (17.d)$$

$$x(j+1) = x(j) + \dot{x}(j) + \frac{1}{2}\ddot{x}(j) + \frac{1}{6}\dddot{x}(j) + \frac{1}{24}\overset{iv}{x}(j) \quad (17.e)$$

Considering $X = [x_{j-2} \quad \dot{x}_{j-2} \quad x_{j-1} \quad \dot{x}_{j-1} \quad x_j \quad \dot{x}_j \quad \ddot{x}_j \quad \dddot{x}_j \quad \overset{iv}{x}_j]^T$ as the state vector, the state matrix

$$\boldsymbol{A}_{SOH} = \begin{bmatrix} 0 & 0 & 1 & 0 & 0 & 0 & 0 & 0 & 0 \\ 0 & 0 & 0 & 1 & 0 & 0 & 0 & 0 & 0 \\ 0 & 0 & 0 & 0 & 1 & 0 & 0 & 0 & 0 \\ 0 & 0 & 0 & 0 & 0 & 1 & 0 & 0 & 0 \\ 0 & 0 & 0 & 0 & 1 & 1 & 1/2 & 1/6 & 1/24 \\ 0 & 0 & 0 & 0 & 0 & 1 & 1 & 1/2 & 1/6 \\ 0 & 0 & 0 & 0 & -p & -d & 0 & 0 & 0 \\ 0 & 0 & p & d & -p & -d & 0 & 0 & 0 \\ -2p & -2d & 4p & 4d & -2p & -2d & 0 & 0 & 0 \end{bmatrix} \quad (18)$$

transfers Eqs. (17) into the state space form.

Investigating the spectral radius of $\boldsymbol{A}_{SOH}$ numerically for different p and d gains, the stability chart can be obtained. Again, if we put zeros in the last and the last two rows of matrix $\boldsymbol{A}_{SOH}$, we will get the same result as having FOHs and ZOHs, respectively. Fig. 6, presents the stability domain of our digitally controlled system using SOH. The maximum p gain is increased significantly (i.e. 0.45) which reduces the minimum steady state error to 55% of the case of ZOH. But the performance of the system is slightly decreased where the least value of the spectral radius of A_{SOH} grows to 0.6929 as opposed to 0.6749 observed in case of ZOH. This shows that the performance and stability cannot be increased unboundedly by using Higher-Order-Holds (HOH). This is discussed in more detail in the next section.

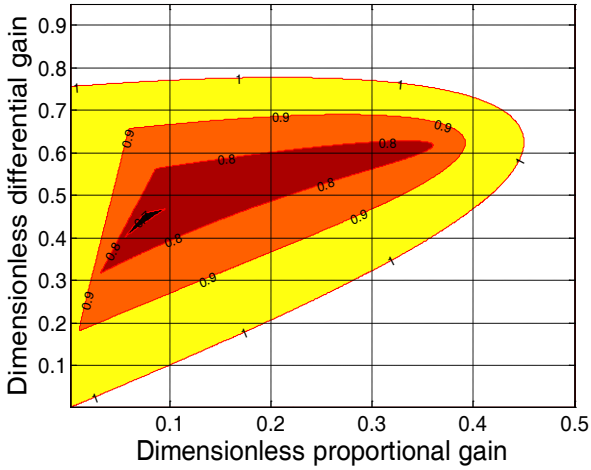

Fig. 6. Stability chart for PD controllers using SOH. The darker colors represent the more stable zones. The maximum allowable dimensionless proportional gain is increased to 0.45, as opposed to 0.25 for the case of using ZOH.

IV. HOH AND THE CONCEPT OF MODIFIED HOLDS

For higher-order holds we can carry out the analysis in a way similar to the cases of FOH and SOH. Table 1 shows the main results of using holds up to the sixth order. It shows that for most applications, the FOH can offer a good performance for the system.

At this stage, let us investigate if any modification can be done to the structure of the controller to improve the performance further. It can be observed that the state space matrix $\boldsymbol{A} \in \mathcal{R}^{3(n+1)\times 3(n+1)}$ of the discrete time system in case of using n-order hold will have the last n rows in the form presented in Table 2, plus n zeros on the right

TABLE 1.

$Q(T)$	p_{max}	Min Spectral Radius	p at min spectral radius
ZOH	0.2500	0.6749	0.0420
FOH	0.3325	0.6657	0.1625
SOH	0.4500	0.6929	0.0525
3rd OH	0.6020	0.7623	0.0490
4th OH	0.5565	0.8365	0.0280
5th OH	0.3675	0.8940	0.0105
6th OH	0.2415	0.9356	0.0070

Main results of using different order holds for PD controllers.

TABLE 2.

Row$_{3(n+1)}$ entries	Even n	Odd n
$a_{1,2}$	$-n![p \quad d]$	$n![p \quad d]$
$a_{3,4}$	$n!\,\lambda_1 n[p \quad d]$	$-n!\,\lambda_2 n[p \quad d]$
$a_{5,6}$	$-n!\,\lambda_3 \sum_{i=1}^{n-1} i\,[p \quad d]$	$n!\,\lambda_4 \sum_{i=1}^{n-1} i\,[p \quad d]$
$a_{7,8}$	$n!\,\lambda_5 \sum_{j=1}^{n-2}(\sum_{i=1}^{j} i)[p \quad d]$	$-n!\,\lambda_6 \sum_{j=1}^{n-2}(\sum_{i=1}^{j} i)[p \quad d]$
$a_{9,10}$	$-n!\,\lambda_7 \sum_{k=1}^{n-3}(\sum_{j=1}^{k}(\sum_{i=1}^{j} i))[p$	$n!\,\lambda_8 \sum_{k=1}^{n-3}(\sum_{j=1}^{k}(\sum_{i=1}^{j} i))[p \quad d]$
⋮	⋮	⋮
⋮	$n!\,\lambda_7 \sum_{j=1}^{n-2}(\sum_{i=1}^{j} i)[p \quad d]$	$n!\,\lambda_6 \sum_{j=1}^{n-2}(\sum_{i=1}^{j} i)[p \quad d]$
⋮	$-n!\,\lambda_5 \sum_{i=1}^{n} i\,[p \quad d]$	$-n!\,\lambda_4 \sum_{i=1}^{n} i\,[p \quad d]$
⋮	$n!\,\lambda_3 n[p \quad d]$	$n!\,\lambda_2 n[p \quad d]$
$a_{2n+4,2n+3}$	$-n!\,\lambda_1[p \quad d]$	$-n![p \quad d]$

The entries of the last n rows of A in case of even and odd n.

side and complementary zeros on the left (for upper rows corresponding to the lower orders). The cofactor λ_m used in Table 2 is defined as: $\lambda_m = \{1 : m < n, 0 : m \geq n\}$. In either case there is an $n!$ coefficient in the rows, which as n grows, makes the matrix more skewed that increases the spectral radius. Actually, this $n!$ comes from the power of time dependent terms in the control force expression. In fact, when a higher order hold is used, the PD structure should be implemented to every corresponding derivative level with the same value of the p and d gains to keep the concept consistent. This would cause to have a coefficient of $1/n!$ beside each level of derivatives as we reach to the acceleration level i.e. the level of control force. In the case of ZOH, there is no level higher than the acceleration level, as the slope and higher derivatives of the state feedbacks are considered zero. We propose to modify the HOH discrete control force to remove the $n!$ coefficient from the rows (see Table 2). This results in:

$$Q_m(T) = -P\left[x(j-1) + \alpha(T-j) + \frac{1}{2!}\alpha'(T-j)^2 + \cdots + \frac{1}{n!}\alpha^{(n-1)'}(T-j)^n\right] - D\left[x'(j-1) + \beta(T-j) + \frac{1}{2!}\beta'(T-j)^2 + \cdots + \frac{1}{n!}\beta^{(n-1)'}(T-j)^n\right] \quad (19)$$

where α and β are defined as the slope of the previous states of the position and velocity respectively. This will not affect the upper rest of the rows of the state space matrix $\boldsymbol{A}$.

After obtaining the spectral radius of the modified matrix $\boldsymbol{A}_m$, for a range of p and d gains, the interesting results of Table 3 is obtained for the first 6 orders of $Q_m(T)$. Of course, the first two orders of $Q_m(T)$ offer the same results as the non-modified $Q(T)$ had.

We can see that with the 4th order modified hold, the system decays at the rate of $e^{(-0.5711)T}$ as apposed to $e^{(-0.6749)T}$ obtained in case of ZOH. This offers more than 10% improvement in performance. Besides, the most robust

TABLE 3.

$Q_m(T)$	p_{max}	Min spectral radius	p at min spectral radius
0 order	0.25	0.6749	0.0420
1st order	0.3325	0.6657	0.1625
2nd order	0.3885	0.6420	0.0840
3rd order	0.3990	0.6096	0.2100
4th order	0.3990	0.5711	0.2170
5th order	0.3990	0.5875	0.2100
6th order	0.3990	0.5884	0.2205

Main results of using different degrees of modified holds for PD controllers.

setting is achieved with $p = 0.217$ which is more than 516% of that of a ZOH, which means more than five times improvement in the best achievable accuracy. For the highest precision, a 4th order modified hold, offers ~60% reduction in the final error, compared to the case of ZOH. The stability domain of the 4th order modified hold is presented in Fig. 7, which itself demonstrates the improvements graphically.

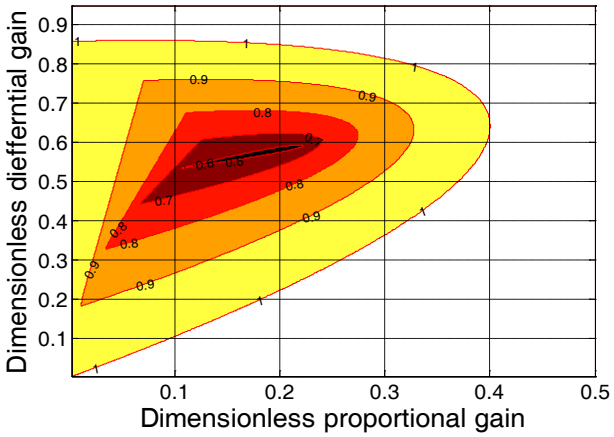

Fig. 7. Stability chart for PD controllers using 4th order modified hold. The darker represent the more stable zones. The most robust zone is situated at $p = 0.21$ and $d = 0.59$.

In the following section, the results are illustrated with computer simulations and experimental tests (please also see the accompanying video).

V. SIMULATIONS AND EXPERIMENTAL RESULTS

Simulink is used to construct the model of our system (see Fig. 2) and check the response of the controlled system to a unit impulse, in case of using ZOH and 4th order modified hold. The state feedbacks are sampled with 100Hz frequency and the mass is considered 1 Kg. As the system operates in the time domain, the defined dimensionless gains, which are functions of the sampling time and system mass, should be converted to ordinary gains. Referring to Fig. 4, for a ZOH, the best achievable robustness is obtained at $p = 0.042$ and $d = 0.32$. The ordinary P and D gains for this system are

$$p = \frac{P\tau^2}{m} \longrightarrow P = \frac{0.042 \times 1}{(0.01)^2} = 420 \ N/m \quad (20)$$

$$d = \frac{D\tau}{m} \longrightarrow D = \frac{0.32 \times 1}{0.01} = 32 \ \ N \cdot s/m \quad (21)$$

After applying these gains to the controller of the simulated system, the behavior shown in Fig. 8 is obtained. As it is shown, the steady state error is 2.38 mm and settling time is around 0.185 sec.

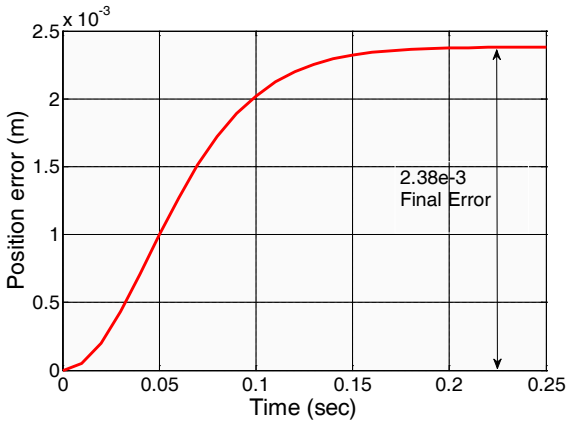

Fig. 8. Behavior of the digitally position controlled system using ZOH, tuned to the most robust setting.

Now we turn to the 4th order modified hold and apply the necessary changes to the control force in the simulation. Employing the same approach, introduced in previous sections, the best achievable performance is obtained numerically at $p = 0.21$ and $d = 0.59$. Keeping the same mass and control frequency the ordinary gains are obtained as $P = 2100$ and $D = 59$. Fig. 9, shows the results after fixing the gains for the new setting. In this case, the settling time is reduced to ~0.175 sec, which is around 10% less than the previous result. Also, as we were expecting, the steady state error is reduced to 0.461mm, which shows ~516% improvement in the accuracy. Some oscillatory behavior can be seen in Fig. 9, which is the result of the considerable increase in virtual stiffness i.e. the proportional gain. The results from the simulations confirm the claims of the paper down to the level of numerical errors.

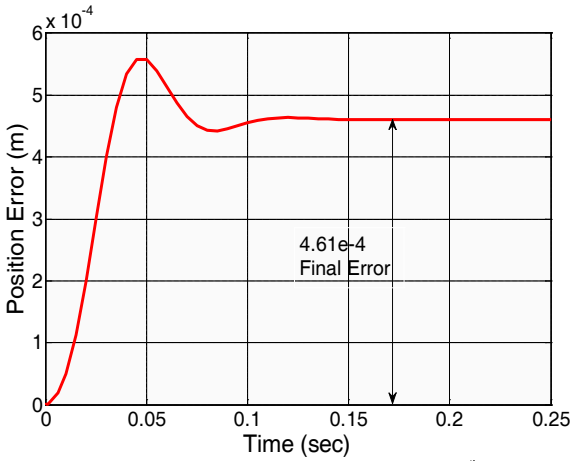

Fig. 9. Behavior of the digitally controlled system using 4th order modified hold, tuned to the most robust setting.

The next stage is to test the concepts on a real physical system to verify the improvements experimentally. For this reason a self-balancing motor-bike robot [4],[5] is used as a position controlled system (see Fig. 10). Ghaffari developed this unique robot in his Master's project work. This robot is equipped with wireless transceivers, which allows us to monitor the behavior of the system in real-time. First of all, the robot was set to its most robust condition using a ZOH.

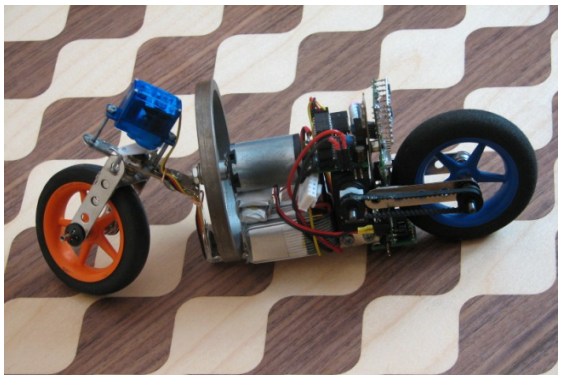

Fig. 10. Self-balancing motor bike robot used for experimental tests.

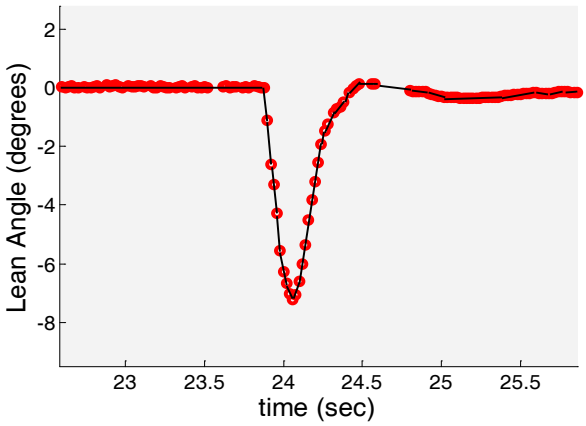

Fig. 11. Behavior of the digitally controlled system using ZOH, tuned for the most robust setting.

The response to an impact (see the accompanying video), captured and recorded and shown in Fig. 11.

A fairly similar behavior (no oscillations) can be observed between the experimental results (Fig. 11) and the simulations (Fig. 8). The settling time is measured around 1 second. We can still increase the proportional gain to improve the accuracy but as we move to the right side in the stability domain (Fig. 4), the robustness is decreased until the border of the chart, where the system starts to oscillate and shows the critical behavior (as also illustrated in the accompanying video). Increasing the proportional gain further will make the system unstable and balancing will not be possible anymore.

For the next step, the 4th order modified hold was implemented on the robot. As we need to generate a non-linear force, probably an analogue circuitry would be the best to drive the actuators, but as we are dealing with a digital controller, it would not be convenient to make the electronic circuits any more complicated. One appropriate solution would be to use the same digital controller to generate piece-wise constant signals (e.g. constant duty ratio PWM signals), at much higher frequencies than that of the control loop (see Fig. 12). This can be done by having two

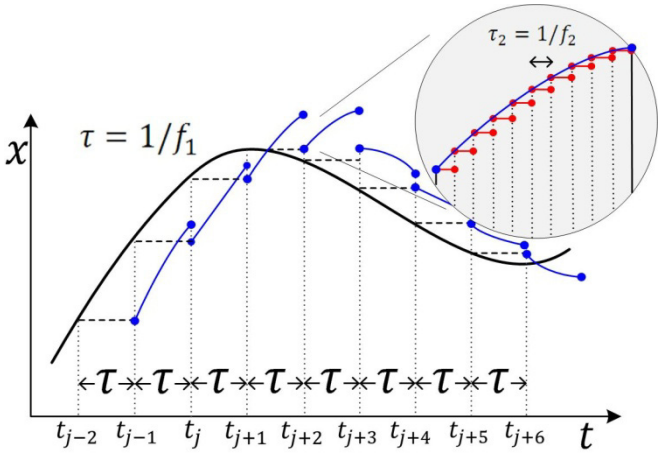

Fig. 12. Illustration of how a non-linear control signal can be constructed with a higher frequency, second digital loop.

different loops in parallel in the control algorithm, one for generating the control signals at the highest possible frequency (f_2 in Fig. 12) and the other for the main control loop at its corresponding frequency (f_1 in Fig. 12).

Parallel loops are supported by many advanced digital chipsets (e.g. multi-core micro controllers, FPGAs, etc.). Even if the processor only supports sequential algorithms, using inner loops would be a next level solution, where the inner loop operates with a high frequency to generate the control force at the end of the main loop. This is due to the fact that in most cases, the physical limitations (e.g. noises, bandwidth of the sensors and amplifiers), introduce much more delay than the CPUs' processing time, so in the meantime the processor can handle the second loop. In the case of our experimental robot, the main controller of the motor-bike operates at 40Hz, however the processor operates at 16MHz. This allows the second loop to generate 500 different control signals in every sampling period which can approximate the required non-linear control signal.

After calibrating the controller for its most robust setting (see Fig. 7), the same impact test as in the previous case was performed. The result showed that the settling time is reduced to 0.91 second (compared to 1 sec for ZOH), which is a 9% improvement. The real-time graph of the robot's response is presented in Fig. 13, which also shows a behavior similar to the simulated model (see Fig. 9).

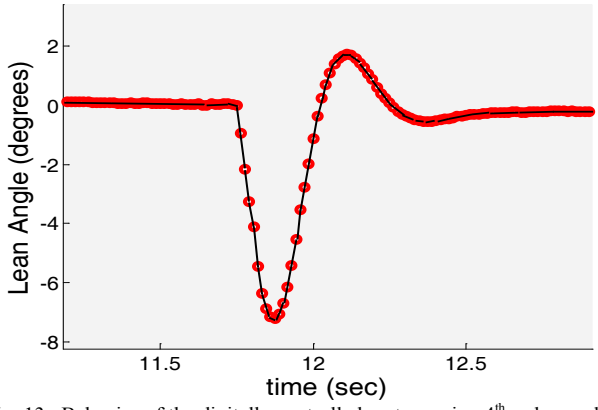

Fig. 13. Behavior of the digitally controlled system using 4th order modified hold, tuned for the most robust setting.

The magnitude of the proportional gain for the 4th order modified hold was more than 5 times of that of the ZOH. This means 80% smaller position error.

These experimental results further confirmed that modified holds improve the performance of digital controllers. This concept is relatively easy to implement and practical. It requires almost no modifications to the hardware of the robot (which could be costly and time consuming). There are many possible fields of industrial applications, where implementing the modified hold can add value and improve the desirable characteristics of the system (e.g. position controlled and haptics).

VI. Conclusion

In this paper, we dealt with possible strategies to improve the stability and performance of computer controlled systems by considering the recent history of the behavior of the system in generating a better control force. The investigation started with implementing first and higher order holds, and ended with the concept of modified holds. The result was a considerable improvement in the accuracy and the performance of the digital control, all at the cost of adding a few more steps to the algorithm of the controller. This modification can be done to many present robots to improve their performance. The improvement also depends on the technical specification of the robot and its nature of use, e.g. we cannot expect any better accuracy than the resolution of the sensors on the robot. Sophisticated control algorithms may demand high-performance processors and more advanced sensors which are often beyond the budget scope of projects.

Most of the investigations were based on the assumption of the availability of actual state feedback, which of course, in practice, needs properly filtered data to obtain approximations for the actual system state.

The presented concepts were illustrated and validated via simulation and experiment. For the experimental testing a novel self-balancing motor bike robot was used.

Acknowledgment

The research work reported here was supported by the Natural Sciences and Engineering Research Council of Canada, Quanser, Inc., and the Canadian Space Agency.
The financial support is gratefully acknowledged.

References

[1] L.L. Kovács, J. Kövecses, G. Stépán, "Analysis of effects of differential gain on dynamic stability of digital force," International Journal of Non-linear Mechanics, 43 (2008) 514 – 520.

[2] T. Kerekes, "Dynamics modeling and control of multi-body systems," M.S. thesis, Budapest University of Technology and Economics. Sep. 2008.

[3] J. Kovacs, "Digital Control Theory," Lecture Notes, Department of Process Engineering, University of Oulu, (1996-2003), pp. 87 – 114.

[4] K. Ghaffari.T, "Design of a self-balancing two wheeled path finder robot," M.S. thesis, Budapest University of Technology and Economics. Sep. 2008.

[5] K. Ghaffari.T, "Design of a self-balancing motor bike robot," IEEE 2008 International Student Experimental Hands-on Project Competition on Intelligent Mechatronics and Automation, Taiwan National University. (received the first prize award)

[6] J. Kövecses, L.L. Kovács, G. Stépán, "Dynamics modeling and stability of robotic systems with discrete-time force control," Archive of Applied Mechanics, 77 (2007) 293 – 299.
[7] M. Jalili kharaajoo, B.N. Araabi, "The Schur stability via the Hurwitz stability analysis using biquadratic transformation," Automatica 41 (2005) 173 – 176.
[8] B. Friedland, "Advanced control system design," Prentice-Hall, (1996) 233 – 306.
[9] T. Insperger, G. Stépán, "Stability improvements of robot control by periodic variation of gain parameters," Proceedings of the 11th World Congress in Mechanism and Machine Science, China Machinery Press, (2004) 1816 – 1820.
[10] T. Insperger, L.L. Kovács, P. Galambos, G. Stépán, "Increasing the accuracy of digital control process using the act-and-wait concept," IEEE/ASME Transactions on Mechatronics, in press (2009).
[11] T. Insperger, G. Stépán, "Optimization of digital control with delay by periodic variation of the gain parameters," IFAC Workshop on Adaptation and Learning in Control and Signal Processing, Yokohama, Japan, Aug. 30 – Sep. 1, 2004
[12] S. Chu, C.C Lin, L.L. Chung, C.C Chang, K.H. Lu, "Optimal performance of discrete-time direct output-feedback structural control with delayed control forces," International Journal of Structural Control and Health Monitoring, (2008) 20 – 42.